

# Thermodynamic Performance and CO<sub>2</sub> Emission Characteristics of Solar-Aided Coal-Fired Power Plant under Off-design Conditions

Hui Yan<sup>1</sup>, Zhu Wang<sup>1</sup>, Meihong Wang<sup>2</sup>, Ming Liu<sup>1</sup>, Daotong Chong<sup>1\*</sup>

<sup>1</sup> State Key Laboratory of Multiphase Flow in Power Engineering, Xi'an Jiaotong University, Xi'an, China.

<sup>2</sup> Department of Chemical and Biological Engineering, University of Sheffield, UK

(\*Corresponding Author: dtchong@mail.xjtu.edu.cn)

## ABSTRACT

Solar-aided coal-fired power plant (SACFPP) is cost-effective to ensure energy security with less CO<sub>2</sub> emission than coal-fired power plant. Its efficient and low-carbon operation is important but difficult because of the time-varying solar energy. This paper evaluates the thermodynamic performance and CO<sub>2</sub> emission characteristics of SACFPP under off-design conditions. Three SACFPP configurations (marked as HP123, HP23 and HP3) were analyzed and the optimized operation strategy is proposed to achieve highest solar-to-power efficiency and lowest CO<sub>2</sub> emission rate through adjusting feedwater ratio to trough collector system. The best achievable solar-to-power efficiency and CO<sub>2</sub> emission rate depend on the power load, DNI, system safety limitation and system configuration. The annual CO<sub>2</sub> emission reductions of the 600 MW SACFPP are about 61352.2, 54009.9 and 51769.8 tonnes under configurations of HP123, HP23 and HP3, respectively. The results can guide the SACFPP operation optimization.

**Keywords:** Solar-aided Coal-fired Power Plant, Off-design condition, CO<sub>2</sub> emission, Solar-to-power efficiency, Process modelling\simulation

## NONMENCLATURE

### Abbreviations

CFPP	Coal-fired power plant
DNI	Direct normal irradiance
OWHE	Oil-water heat exchanger
PTC	Parabolic trough collector
SACFPP	Solar-aided coal-fired power plant
TCS	Trough collector system

### Symbols

$h$	Enthalpy, kJ kg <sup>-1</sup>
$Q$	Transferred heat, kJ
$\eta$	Efficiency, %

## 1. INTRODUCTION

The global energy structure is becoming lower-carbon, more efficient, clean and diversified. Renewable energy has been growing significantly in recent years[1]. According to the BP Statistic Review of Energy 2022[2], wind and solar power first reached 10.2% of the global power generation in 2021. However, a large amount of renewable power such as photovoltaics and wind power connecting to grid brings difficulties for power grid stability. Traditional fossil power plants are still required to guarantee the power stability. Coal-fired power nowadays still dominates the power sector of some developing countries such as China, but its carbon dioxide (CO<sub>2</sub>) emission is very serious from the environmental view. Therefore, coal-fired power plant (CFPP) should be reformed to not only ensure energy security but also significantly reduce the CO<sub>2</sub> emission.

Solar-aided coal-fired power system (SACFPP) is a cost-effective and low-carbon technology to address the issue mentioned above. It can reduce the cost of concentrated solar power by sharing the turbines and removing energy storage in CSP while the intermittency of solar energy can be compensated by CFPP[3]. Most importantly, the coal consumption and CO<sub>2</sub> emission in CFPP can be reduced by solar integration.

In SACFPP, solar energy can be integrated into the CFPP by heating feedwater[4, 5], condensate water[6], or steam[7]. Many in-depth studies have been conducted on the SACFPP system design, optimization and off-design performance in energy and exergy aspects. For system design, Qin et al.[8] compared annual solar-to-power efficiency and solar share in four

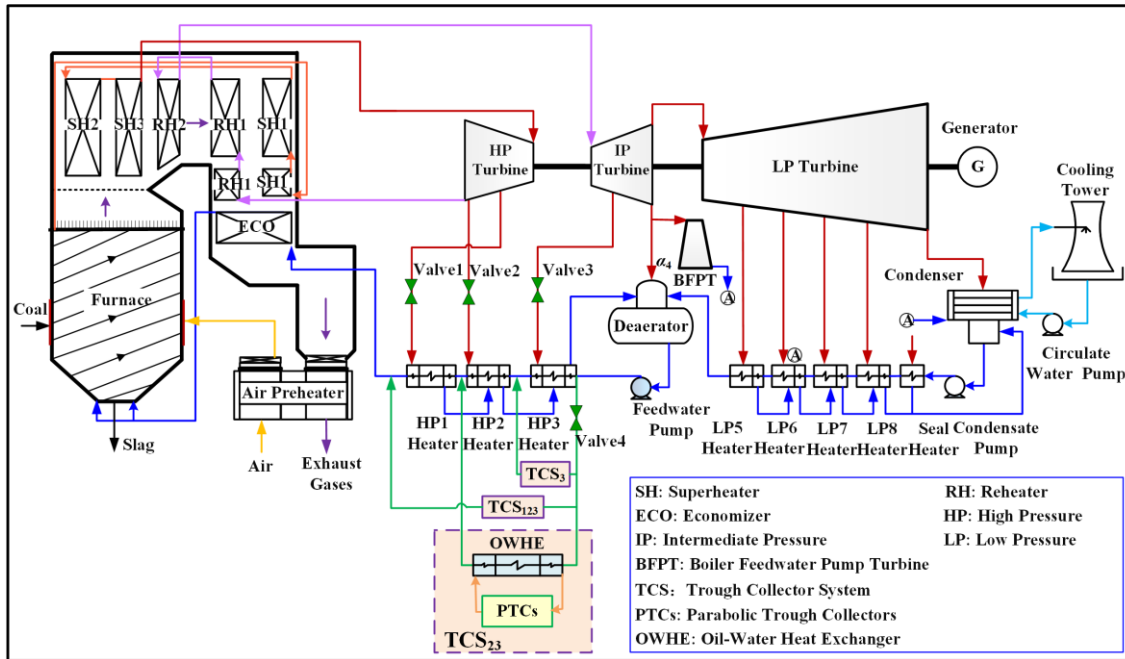


Fig. 1. Configurations of SACFPP

configurations with solar heater connecting in parallel or in series with the regenerative heaters. Shagdar et al.[9] examined the integration mechanism of solar energy into a 300 MW CFPP including replacing part of the steam extractions from turbines. Zhong et al.[10] proposed a changeable integration mode according to the direct normal irradiance (DNI) to achieve the minimum levelized electricity cost. As for performance analysis, Li et al.[11] developed an all-condition mechanism model for SACFPP, and simulated the system in power booting mode and fuel saving mode; solar-to-power efficiency is about 2-3% higher in the former mode. Adibhatla et al.[12] conducted exergy and thermo-economic analyses of a 500 MW SACFPP, and the results revealed that exergy destruction of boiler and solar field were two main sources of system irreversibility. Zhu et al.[13] analyzed the exergy distribution of a solar-tower-aided coal-fired power plant.

Due to the time-varying characteristics of solar energy, SACFPP needs to operate in off-design modes for a long time. The SACFPP performance in off-design modes should also be clarified from the environmental aspect. The efficient and environmental-friendly operation of SACFPP is very important but difficult, which has not been fully discussed in previous studies.

This study aims to investigate the thermodynamic performance and CO<sub>2</sub> emission characteristics of a SACFPP in off-design conditions. Models of SACFPP are developed including CFPP, trough collector system (TCS) and solar-coal integration. The energy conversion and

CO<sub>2</sub> emission characteristics under different DNIs, loads and with three configurations are obtained. Finally, the operation strategy to achieve efficient and environmental-friendly is proposed.

## 2. MODEL DEVELOPMENT AND VALIDATION

### 2.1 Configuration of SACFPP

As shown in Fig.1, the SACFPP is composed of a reference CFPP and TCS. The solar energy is absorbed in TCS and then integrated into the CFPP by replacing part of the steam extractions. The saved steam continuous expanding in the turbines and generates extra power.

The TCS consists parabolic trough collectors (PTCs) and the oil water heat exchanger (OWHE). The thermal oil is heated in PTCs and flows into the OWHE to transfer heat to the water. The reference CFPP is a supercritical 600 MW CFPP. Taking account of the feasibility, convenience and efficiency of the retrofitting CFPP, the TCS should operate in parallel with one or several consecutive HP heaters. Thus, three configurations are considered in this paper: 1) TCS in parallel with three high-pressure (HP) heaters (marked as HP123); 2) TCS in parallel with HP2 and HP3 (marked as HP23); 3) TCS in parallel with HP3 (marked as HP3).

### 2.2 Models of TCS and CFPP

PTC and OWHE are two key components of the TCS system. The oil output/input of PTC are connected with the oil input/output of OWHE, respectively. Solar energy

heats the water indirectly, which is achieved by heating the oil in PTC directly and the heated oil transferring heat to the water in OWHE. The operation parameters of CFPP steam turbines under off-design conditions can be calculated based on the Flugel formula[14, 15].

### 2.3 Model of solar-coal integration

In the SACFPP, the model of the solar integration is developed to indicate the influence of solar integration on the CFPP operational parameters. Feedwater ratio to TCS is used to describe the ratio of feedwater mass flowrate heated by TCS over the total feedwater mass flowrate. Its mathematical formula is shown as:

$$\beta_{TCS} = \frac{m_{wTCS}}{m_{wtot}} \quad (1)$$

where,  $\beta_{TCS}$  is the feedwater ratio to TCS;  $m_{wTCS}$  is the feedwater mass flowrate heated by TCS,  $\text{kg}\cdot\text{s}^{-1}$ ; and  $m_{wtot}$  is the total feedwater mass flowrate,  $\text{kg}\cdot\text{s}^{-1}$ .

Supposing the water heated by TCS and HP heaters is mixed at input of HP( $i-1$ ) heaters, the enthalpy of the water mixture is calculated with:

$$h_{w(i-1)in} = \beta_{TCS} \times h_{sout} + (1 - \beta_{TCS}) h_{wiout} \quad (2)$$

where,  $h_{w(i-1)in}$  is the input water enthalpy of HP( $i-1$ ) heater,  $\text{kJ}\cdot\text{kg}^{-1}$ ;  $h_{sout}$  is the output water enthalpy of OWHE,  $\text{kJ}\cdot\text{kg}^{-1}$ ;  $h_{wiout}$  is the output water enthalpy of HP $i$  heater,  $\text{kJ}\cdot\text{kg}^{-1}$ .

## 3. METHOD FOR THERMODYNAMICS AND CO<sub>2</sub> EMISSION ANALYSIS

### 3.1 Indicators for thermodynamic performance analysis

Solar-to-power efficiency describes the energy conversion ability of SACFPP from the solar thermal energy to electricity[16]. Its calculation method can be written as:

$$\eta_{SP} = \frac{W_{add}}{Q_{sun}} \times 100\% \quad (3)$$

where  $\eta_{SP}$  is the solar-to-power efficiency, %;  $W_{add}$  is the additional power generated by SACFPP compared with CFPP (consuming same amount of coal), kW;  $Q_{sun}$  is the absorbed solar energy, kJ.

Standard coal consumption rate of SACFPP ( $b_{ACR}$ ) is calculated with:

$$b_{ACR} = \frac{3600 \cdot Q_b}{q_{a-net} \eta_b \eta_p W_{SC}} \times 1000 \quad (4)$$

where  $Q_b$  is the boiler heat absorption, kW;  $q_{a-net}$  is the low heating value of the standard coal,  $\text{kJ}\cdot\text{kg}^{-1}$ ;  $\eta_b$  is the boiler efficiency, assumed as 93.7%;  $\eta_p$  is the pipe efficiency, assumed as 98%;  $W_{SC}$  is the power generation of the SACFPP, kW.

Saved standard coal consumption rate ( $\Delta b_{ACR}$ ) describes the coal consumption reduction of SACFPP compared with CFPP if the power generation is same.

$$\Delta b_{ACR} = b_{ACR} - b_{ACR,CF} \quad (5)$$

where,  $b_{ACR,CF}$  is the standard coal consumption rate of CFPP with the same power generation as SACFPP,  $\text{g}\cdot\text{kWh}^{-1}$ .

### 3.2 Indicators for CO<sub>2</sub> emission analysis

SACFPP can greatly reduce the pollutant emissions, especially CO<sub>2</sub>. The CO<sub>2</sub> emission rate, the CO<sub>2</sub> emission reduction rate and the equivalent annual CO<sub>2</sub> emission reduction are applied to analyze carbon reduction effect.

The CO<sub>2</sub> emission rate is calculated from the coal consumption and characteristics of the fired coal. Its mathematical formula is shown as:

$$b_{CO_2,g} = b_{ACR} \times C_{ar} (1 - Q_4) \times \frac{44}{12} \times \frac{q_{a-net}}{q_{net}} \quad (6)$$

where,  $b_{CO_2,g}$  is the CO<sub>2</sub> emission rate for 1 kWh power generation by SACFPP,  $\text{g}\cdot\text{kWh}^{-1}$ ;  $C_{ar}$  is the mass fraction of carbon on as-received basis of the fired coal, %;  $Q_4$  is the heat loss due to unburned solid combustibles,  $\text{kJ}\cdot\text{kg}^{-1}$ ;  $q_{net}$  is the low heating value of the fired coal,  $\text{kJ}\cdot\text{kg}^{-1}$ .

CO<sub>2</sub> emission reduction rate compared with CFPP is:

$$\Delta b_{CO_2,g} = b_{CO_2,g} - b_{CO_2,gCF} \quad (7)$$

where,  $\Delta b_{CO_2,g}$  is the CO<sub>2</sub> emission reduction rate of SACFPP compared with the CFPP,  $\text{g}\cdot\text{kWh}^{-1}$ ;  $b_{CO_2,gCF}$  is the CO<sub>2</sub> emission rate of CFPP,  $\text{g}\cdot\text{kWh}^{-1}$ .

The equivalent annual CO<sub>2</sub> emission reduction is estimated by the design power output, the maximum CO<sub>2</sub> emission reduction rate at 100%THA, and the effective working hours in a year (8760 hours) at which the CFPP operates at design power output. The equivalent annual CO<sub>2</sub> emission reduction is calculated with:

$$\Delta b_{CO_2,ann} = \max(\Delta b_{CO_2,g}) \Big|_{100\%THA} \cdot t_{EWH} \cdot W_{CFref} \cdot 10^{-6} \quad (8)$$

where,  $\Delta b_{CO_2,ann}$  is the equivalent annual CO<sub>2</sub> emission reduction, tonne year<sup>-1</sup>;  $t_{EWH}$  is the effective working hour, h year<sup>-1</sup>, whose calculation is referred in reference [17];  $W_{CFref}$  is the design power output of CFPP, kW.

## 4. RESULTS AND DISCUSSION

### 4.1 Case description

The design power output of the reference CFPP is 600322 kW. The design DNI is 700  $\text{W}\cdot\text{m}^{-2}$ . In a typical year, the total solar irradiance is about 1543.6 kWh and the maximum DNI is 1064  $\text{W}\cdot\text{m}^{-2}$ . After calculation with the method in reference [17], the effective working hour is 2073 hour. Table 1 shows the structures data about TCS.

Table 1: Structures data about the TCS

Parameter	Value	Parameter	Value
Length of PTC unit/m	47.1	Length of OWHE unit /m	2.6
Outer diameter of absorber /m	0.07	Numbers of PTC/OWHE units in series	10
Inner diameter of absorber /m	0.066	Reflector opening Width/m	5
Outer diameter of glass tube /m	0.115	Inner diameter of OWHE tube /m	0.015
Inner diameter of absorber /m	0.109	Outer diameter of OWHE tube /m	0.019
Number of PTC in parallel	80	Inner diameter of OWHE shell /m	0.9
Number of PTC units in series	10	Number of OWHE units in parallel	1500

## 4.2 Performance under different conditions

### 4.2.1 Performance of HP123 under different DNIs

Thermodynamic performance and CO<sub>2</sub> emission characteristics of SACFPP depend on the system configuration, DNI, power load and feedwater ratio to TCS. Taking the configuration of HP123 as an example, analyses are conducted with different DNIs at 100%THA.

As shown in Fig.2, the OWHE output water enthalpy increases with DNIs while decreases with the increase of the feedwater ratio to TCS. In order to guarantee the operation safety, the OWHE output water enthalpy should be lower than the water enthalpy of the 340 °C at the pressure of feedwater (dotted line in Fig.2). The lowest allowed feedwater ratio to TCS is shown in Table 2, ranging in 0.1 – 0.25 for DNI of 300 – 700 W m<sup>-2</sup>.

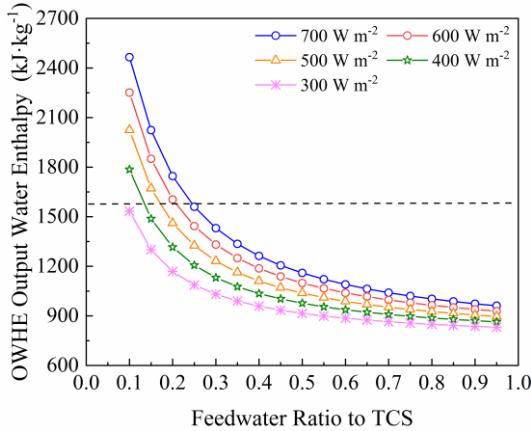


Fig.2 OWHE output water enthalpy in HP123 under 100%THA with different DNIs

Table 2 Lowest allowed feedwater ratios to TCS

DNI (W m <sup>-2</sup> )	300	400	500	600	700
Lowest allowed $\beta_{TCS}$	0.1	0.15	0.2	0.25	0.25

As shown in Fig.3, the solar-to-power efficiency changing tendencies are similar under different DNIs. They increase with DNI but have maximum values,

whereas the achievable maximum solar-to-power efficiency also depends on the lowest allowed feedwater ratio to TCS. Therefore, when DNI ranges in 300 - 700 W m<sup>-2</sup>, the achievable maximum solar-to-power efficiency ranges in 26.4% -29.2% with the feedwater ratio to TCS at lowest allowed value.

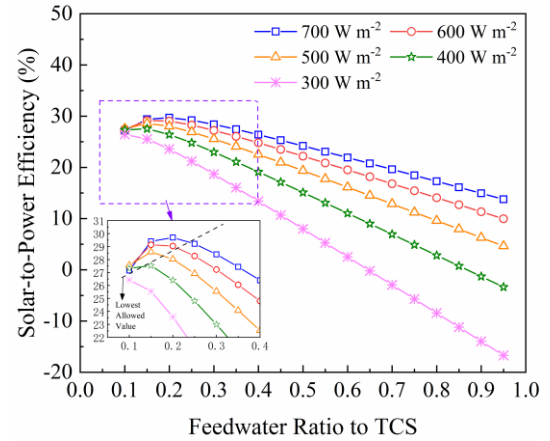


Fig.3 Solar-to-power efficiency in HP123 under 100%THA with different DNIs

The standard coal consumption of the reference CFPP at 100%THA is 284.8 g kWh<sup>-1</sup>. As shown in Fig.4, when DNI is higher than 500 W m<sup>-2</sup>, all the standard coal consumption rates of SACFPP are lower than those of CFPP, while when DNI is lower than 500 W m<sup>-2</sup>, they may be higher than those of CFPP when feedwater ratio to TCS is high. The reason is that the solar energy is insufficient to heat such amount of the feedwater whilst the thermal energy with high energy degree in boiler has to make up energy insufficiency. Besides, Fig.4 also shows that the standard coal consumption rate first decreases and then increases with the feedwater ratio to TCS increasing. The lowest achievable standard coal consumption rate depends on the DNI and the lowest allowed feedwater to TCS. The lowest standard coal consumption rate is 267.4 g kWh<sup>-1</sup> under 700 W m<sup>-2</sup> DNI. The maximum saved standard coal consumption can be achieved by adjusting feedwater ratio to TCS. Integrating solar energy in such case can reduce the coal consumption at most 17.4 g kWh<sup>-1</sup> comparing to CFPP.

As shown in Fig.5, the CO<sub>2</sub> emission rate of SACFPP has similar tendency as the standard coal consumption rate. It first decreases and then increases with the increase of feedwater ratio to TCS. Theoretically, feedwater ratio to TCS has the best value to achieve the minimum CO<sub>2</sub> emission rate, but the achievable minimum CO<sub>2</sub> emission rate also depends on the lowest allowed feedwater ratio to TCS, increasing with the DNI decreasing. Comparing with CFPP in 100%THA, SACFPP has the maximum CO<sub>2</sub> emission reduction rate ranging in 19.4 - 49.3 g kWh<sup>-1</sup> when DNI in 300 - 700 W m<sup>-2</sup>.

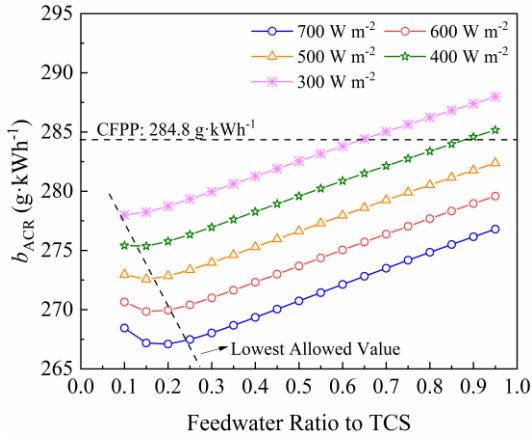


Fig.4 Standard coal consumption rates in HP123 under 100%THA with different DNIs

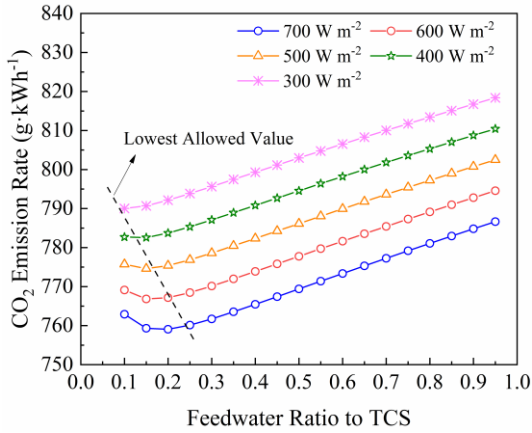


Fig.5 CO<sub>2</sub> emission reduction rates in HP123 under 100%THA with different DNIs

#### 4.2.2 Performance under different power loads

The performance of SACFPP in HP123 configuration under 100%THA, 75%THA and 50%THA are analyzed with 700 W m<sup>-2</sup> DNI. The solar-to-power efficiency and CO<sub>2</sub> emission characteristics are compared in Fig.6 and Fig.7.

As shown in Fig.6, solar-to-power efficiency has the maximum value in every power load condition, but the achievable maximum value is also limited by the lowest allowed feedwater ratio to TCS for system operation safety. In addition, when the feedwater ratio to TCS is lower than 0.25, solar-to-power efficiency increases with the power load, because the OWHE heat load may be less than the absorbed solar energy and it decreases with the power load. When the feedwater ratio to TCS is not lower than 0.3, solar-to-power efficiency decreases with the power load because the boiler inlet water temperature after solar integration increases with the power load decreasing. The max achievable solar-to-power efficiency ranges in 29.2% -30.6%.

As shown in Fig.7, CO<sub>2</sub> emission rate decreases with the power load, and the CO<sub>2</sub> emission reduction rate (compared with CFPP) increases with the power load,

because the boiler heat absorption reduction decreases with power load when the same amount of solar energy is integrated. The achievable maximum CO<sub>2</sub> emission rates are 760.1 g kWh<sup>-1</sup>, 748.9 g kWh<sup>-1</sup>, 723.9 g kWh<sup>-1</sup>, reduced by 49.3 g kWh<sup>-1</sup>, 66.9 g kWh<sup>-1</sup>, 103.0 g kWh<sup>-1</sup> compared to the CFPP, when feedwater ratio to TCS is 0.25, 0.35 and 0.5 under 100%THA, 75%THA and 50%THA, respectively.

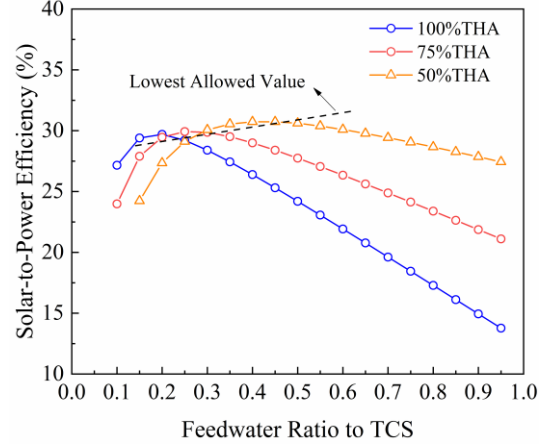


Fig.6 Solar-to-Power efficiency in HP123 configuration under different loads

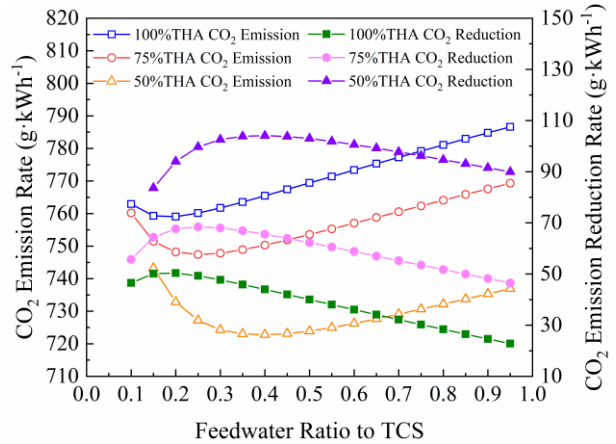


Fig.7 CO<sub>2</sub> Emission characteristics in HP123 configuration under different loads

#### 4.3 Performance under different configurations

This section analyzes the solar energy conversion and CO<sub>2</sub> emission characteristics of SACFPP in different configurations with the same TCS structure. Simulations of SACFPP in HP123, HP23 and HP3 configurations are conducted under 100%THA with the design DNI (700 W m<sup>-2</sup>). Performance is shown in Fig.8 and Fig.9.

As shown in Fig. 8, the solar-to-power efficiencies in three configurations all first increase then decrease with the increase of the feedwater ratio to TCS, and the highest value decreases with the number of HP heaters that TCS is replaced. Maximum achievable values are achieved when feedwater ratio to TCS is at its lowest

allowed value which is 0.25. The highest achievable solar-to-power efficiencies are 29.2%, 26.2% and 25.0% for HP123, HP23 and HP3, respectively. Feedwater ratio to TCS should be adjusted to its lowest allowed value to have best energy conversion characteristics of SACFPP.

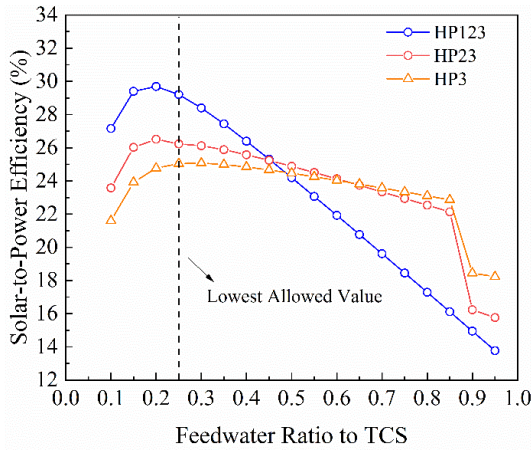


Fig.8 Solar-to-power efficiencies in three configurations under 100%THA with  $700 \text{ W m}^{-2}$  DNI

Compared to CFPP under 100%THA, The  $\text{CO}_2$  emission reduction rates are shown in Fig.9. In every configuration, it has the theoretical maximum value but the achievable largest value is also limited by the lowest allowed feedwater ratio to TCS, which is determined by the operation safety. The achievable maximum  $\text{CO}_2$  emission reduction rate increases with the number of HP heaters that TCS is replaced. They are  $49.3 \text{ g kWh}^{-1}$ ,  $43.4 \text{ g kWh}^{-1}$ , and  $41.5 \text{ g kWh}^{-1}$  in HP123, HP23 and HP3, respectively. Besides, when the feedwater ratio to TCS is larger than 0.45, HP123 is no longer the configuration that reduces the most  $\text{CO}_2$  emission, because the solar energy is not enough to heat the water to the same temperature as output water temperature of HP1 heater. The sudden decreases of  $\text{CO}_2$  emission reduction rate in HP23 and HP3 configuration are caused by the shutdown of HP2 heater or HP3 heater.

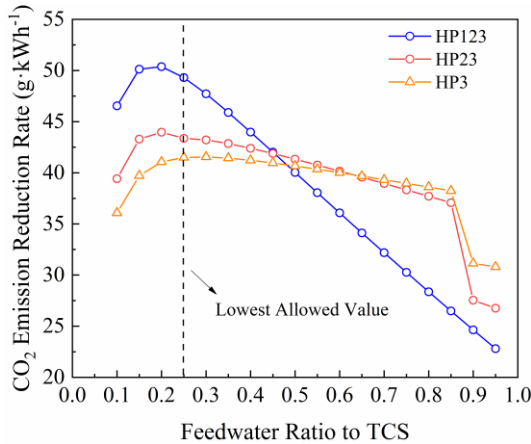


Fig.9  $\text{CO}_2$  emission reduction rate in three configurations

The equivalent annual  $\text{CO}_2$  emission reductions of the three configurations are shown in Table 3. The maximum reduction in  $\text{CO}_2$  emission is obtained for SACFPP with all HP heaters are replaced (Configuration HP123), which is  $61352.2 \text{ tonne}\cdot\text{year}^{-1}$ , while the minimum reduction is  $51769.8 \text{ tonne}\cdot\text{year}^{-1}$  for SACFPP with only HP3 replacement.

Configuration	HP123	HP23	HP3
$W_{\text{CFref}}$ (kW)	600322	600322	600322
$\max(\Delta b_{\text{CO}_2, \text{g}})  _{100\% \text{THA}}$ ( $\text{g}\cdot\text{kWh}^{-1}$ )	49.3	43.4	41.6
$t_{\text{EWH}}$ ( $\text{h year}^{-1}$ )	2073	2073	2073
$\Delta b_{\text{CO}_2, \text{ann}}$ ( $\text{tonne year}^{-1}$ )	61352.2	54009.9	51769.8

#### 4.4 Operation Strategy

According to the off-design performance of SACFPP under different DNIs, loads and configurations. It can be deduced that feedwater ratio to TCS is the key parameter to control SACFPP operation. Adjusting feedwater ratio to TCS can achieve highest solar-to-power efficiency and lowest  $\text{CO}_2$  emission rate. The best feedwater ratio to TCS is either the lowest allowed value or the value that has maximum solar-to-power efficiency and minimum  $\text{CO}_2$  emission rate. Under high power load conditions, the best achievable value is always at lowest allowed feedwater ratio to TCS when DNI is high. When DNI is low, it depends on the power load and the system configuration.

### 5. CONCLUSIONS

Solar-aided coal-fired power generation is a low-carbon solution to overcome intermittency of solar energy. This study investigates the thermodynamic performance and  $\text{CO}_2$  emission characteristics under off-design conditions. The first-principle off-design model of SACFPP was developed and validated. The influences of DNIs, power loads and system configurations on the off-design performance of SACFPP were analyzed. Moreover, the operation strategy to achieve lowest  $\text{CO}_2$  emission and highest solar-to-power efficiency is proposed. The main conclusions are as follows:

(1) Solar-to-power efficiency increases with the DNI and it first increases and then decreases with the increase of feedwater ratio to TCS. The achievable maximum solar-to-power efficiency depends on the DNI, power loads and the lowest allowed feedwater ratio to TCS. In configuration of HP123, the achievable maximum solar-to-power efficiency ranges in 26.4% -29.2% when the DNI ranges in  $300 - 700 \text{ W m}^{-2}$ .

(2)  $\text{CO}_2$  emission rate has minimum values in different loads and DNIs. The minimum  $\text{CO}_2$  emission

rate increases with the decrease of DNI. The achievable minimum CO<sub>2</sub> emission rate depends on the DNI, power loads and the lowest allowed feedwater ratio to TCS which is decided by the system operation safety. Comparing to the CO<sub>2</sub> emission rate of CFPP in 100%THA, the maximum CO<sub>2</sub> emission reduction rate ranges in 19.4 - 49.3 g kWh<sup>-1</sup> when DNI ranging in 300 - 700 W m<sup>-2</sup> under configuration of HP123.

(3) The equivalent annual CO<sub>2</sub> emission reduction increases with the number of HP heaters that TCS is replaced. It can avoid approximately 61352.2 tonne, 54009.9 tonne and 51769.8 tonne CO<sub>2</sub> emission under configurations of HP123, HP23 and HP3, respectively.

(4) Adjusting feedwater ratio to TCS can achieve best solar-to-power efficiency and lowest CO<sub>2</sub> emission rate. The best values depend on the DNI, power load, system configuration and the system safety limitation.

#### ACKNOWLEDGEMENT

This work was supported by the National Natural Science Foundation of China (Grant Number 52306022) and the National Key Research and Development Program of China (Grant Number 2022YFB4202403). The UK author would like to thank the financial support of the EU RISE project OPTIMAL (Grant Agreement No: 101007963).

#### DECLARATION OF INTEREST STATEMENT

The authors declare that they have no known competing financial interests or personal relationships that could have appeared to influence the work reported in this paper. All authors read and approved the final manuscript.

#### REFERENCE

[1] Ding Y, Olumayegun O, Chai Y, Liu Y, Wang M. Simulation, energy and exergy analysis of compressed air energy storage integrated with organic Rankine cycle and single effect absorption refrigeration for trigeneration application. *Fuel*. 2022;317.

[2] BP. *bp Statistical Review of World Energy*. 2022.

[3] Pierce W, Gauché P, Theodor vB, Brent AC, Tadros A. A comparison of solar aided power generation (SAPG) and stand-alone concentrating solar power (CSP): A South African case study. *Appl Therm Eng*. 2013;61(2):657-62.

[4] Li JL, Yu XC, Wang JZ, Huang SH. Coupling performance analysis of a solar aided coal-fired power plant. *Appl Therm Eng*. 2016;106:613-24.

[5] Ahmadi G, Toghraie D, Akbari OA. Solar parallel feed water heating repowering of a steam power plant: A case study in Iran. *Renewable and Sustainable Energy Reviews*. 2017;77:474-85.

[6] Wang F, Li HL, Zhao J, Deng S, Yan JY. Technical and economic analysis of integrating low-medium temperature solar energy into power plant. *Energ Convers Manage*. 2016;112:459-69.

[7] Suojanen S, Hakkarainen E, Tähtinen M, Sihvonen T. Modeling and analysis of process configurations for hybrid concentrated solar power and conventional steam power plants. *Energ Convers Manage*. 2017;134:327-39.

[8] Qin JY, Hu E, Nathan GJ. The performance of a Solar Aided Power Generation plant with diverse "configuration-operation" combinations. *Energ Convers Manage*. 2016;124:155-67.

[9] Shagdar E, Shuai Y, Lougou BG, Mustafa A, Choidorj D, Tan HP. New integration mechanism of solar energy into 300 MW coal-fired power plant: Performance and techno-economic analysis. *Energy*. 2022;238:122005.

[10] Zhong W, Chen XB, Zhou Y, Wu YL, Lopez C. Optimization of a solar aided coal-fired combined heat and power plant based on changeable integrate mode under different solar irradiance. *Sol Energy*. 2017;150:437-46.

[11] Li JL, Xin Y, Hu B, Zeng K, Wu ZY, Fan SW, et al. Safety and thermal efficiency performance assessment of solar aided coal-fired power plant based on turbine steam double reheat. *Energy*. 2021;226:120277.

[12] Adibhatla S, Kaushik SC. Exergy and thermoeconomic analyses of 500 MWe sub critical thermal power plant with solar aided feed water heating. *Appl Therm Eng*. 2017;123:340-52.

[13] Zhu Y, Zhai RR, Peng H, Yang YP. Exergy destruction analysis of solar tower aided coal-fired power generation system using exergy and advanced exergetic methods. *Appl Therm Eng*. 2016;108:339-46.

[14] Yan H, Li X, Liu M, Chong D, Yan J. Performance analysis of a solar-aided coal-fired power plant in off-design working conditions and dynamic process. *Energ Convers Manage*. 2020;220:113059.

[15] Yan H, Liu M, Wang Z, Zhang K, Chong D, Yan J. Flexibility enhancement of solar-aided coal-fired power plant under different direct normal irradiance conditions. *Energy*. 2023;262:125349.

[16] Yan H, Liu M, Chong D, Wang C, Yan J. Dynamic performance and control strategy comparison of a solar-aided coal-fired power plant based on energy and exergy analyses. *Energy*. 2021;236:121515.

[17] Adibhatla S, Kaushik SC. Energy, exergy, economic and environmental (4E) analyses of a conceptual solar aided coal fired 500 MWe thermal power plant with thermal energy storage option. *Sustain Energy Technol*. 2017;21:89-99